

BCAL Test Module - Studies with Cosmic Rays

Alex R. Dzierba

Introduction

This note summarizes some analyses of the cosmic ray data collected during the September 2006 test run of the BCAL module in Hall B. A more detailed analysis of the cosmic ray data is being carried out by the GlueX group from the University of Athens. This note concentrates on using cosmic ray data to understand relative gain settings among the 36 PMT's associated with the 18 BCAL segments. A comparison with a simple Monte Carlo simulation is also presented.

Seen from an end of the BCAL module, each readout *segment* is 3.81×3.81 cm² in area. There are three rows along the vertical direction and six columns along the horizontal direction. The sum of the PMT's associated with a row is called a *sector* and there are three sectors (top-middle-bottom) and the sum of the PMT's associated with a column is called a *layer* and there are six layers labeled 1 through 6. For the most part cosmic rays enter the top sector and exit the bottom sector. For beam runs, a photon incident at 90° enters layer 1 and initiates a shower that exits through layer 6. Thus the photon sees 23 cm of the Pb/SciFi matrix while the cosmic ray sees half that. A schematic of the readout is shown in Figure 1.

Two cosmic ray scintillation counters (paddles) were used for the beam tests. The two cosmic ray paddles were each 10×40 cm² and were oriented with their long side perpendicular to the BCAL module. One paddle was located ≈ 2.5 cm above the top sector and the other was located ≈ 7.5 cm below the bottom sector of the BCAL module. The mid-point of the long dimension of the paddles was located between layers 3 and 4 of the BCAL module.

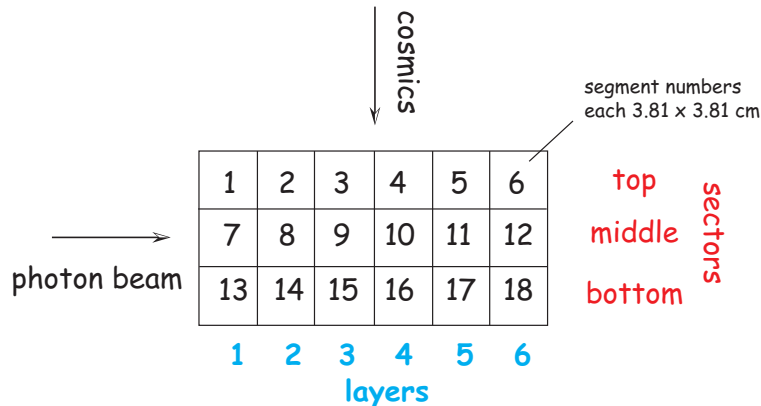


Figure 1: BCAL module readout arrangement at each end. The PMT's associated with layers 1 through 3 are readout using 18 XP2020 PMT's and layers 4 through 6 use Burle PMT's.

Data Runs

Cosmic ray data from five runs were analyzed and these are listed in Table 1. The data files used have ADC and TDC values for each PMT. The ADC and TDC numbers have been processed – the pedestals have been subtracted for ADC values.

Table 1: Cosmic ray runs analyzed. The z -position refers to the position of the paddles along the BCAL module where $z = 0$ is the center and positive z is towards the North end of the module.

Run number	z -position (cm)	Number of Events.
2476	-150	23,724
2475	-50	29,713
2538	0	1,592
2458	+100	33,252
2459	+150	46,593

Preliminary ADC Spectra

Several methods can be used to combine the North and South PMT's ADC information. One is to simply sum the ADC information from the 36 PMT's. Another is to sum the ADC's for the North end and South end separately and then take their geometric mean and multiply by two. Yet another is to sum twice the geometric mean of the two ADC's for each of the 18 segments and add the resulting numbers. The results of the three methods are shown in Figure 2 where the methods are labeled *sum*, *mean1* and *mean2* respectively. The sums are shown for the runs with paddles located at $z = -150$ cm and $z = +150$ cm.

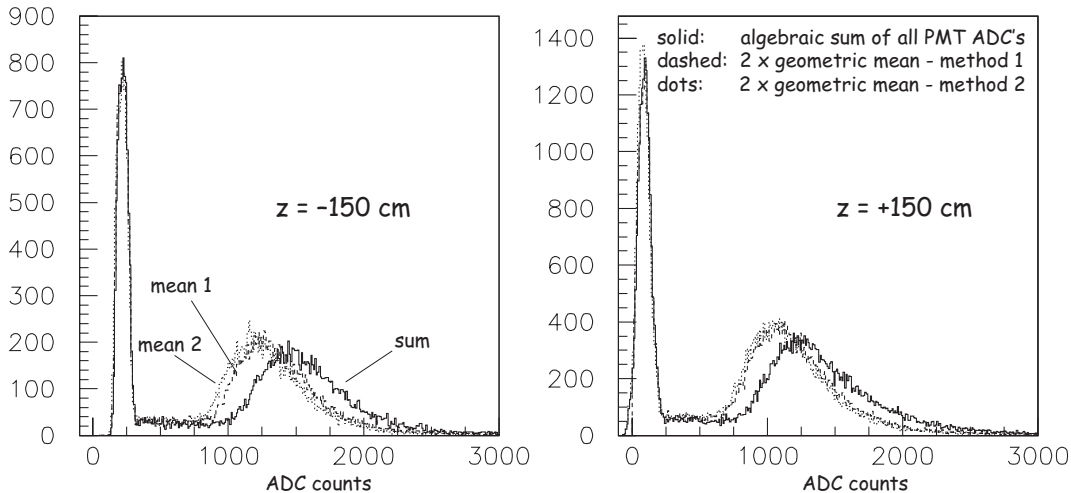


Figure 2: The ADC spectra for cosmic ray runs with $z = \pm 150$ cm combining the 36 ADC's in various ways as described in the text.

Let us assume that the gains of the North and South PMT/ADC are balanced. Then for a light source located at z , as measured from the middle of the BCAL module of length L the sum of the signals from the North and South ends is proportional to $e^{-L/2\lambda}(e^{+z/\lambda} + e^{-z/\lambda})$ where λ is the attenuation length while twice the geometric mean is proportional to $2e^{-L/2\lambda}$. In the middle ($z = 0$) the sum and twice the geometric mean are the same. For z/λ small, the ratio of algebraic sum to twice the geometric mean goes like $z^2/2\lambda^2$. In our case we assume $L = 400$ cm and $\lambda = 257$ cm.

If we assume that there is a factor between North and South gains, for example $g_S = \alpha g_N$ then the ratio of the sum to twice the geometric mean is R as given in equation 1.

$$R = \frac{e^{+z/\lambda} + \alpha e^{-z/\lambda}}{2\sqrt{\alpha}} \quad (1)$$

The ratio of the algebraic sum to twice the geometric sum for the North and South sums for the five runs listed in Table 1 are shown in Figure 3. The curve is a fit to equation 1 with α given by 1.07 ± 0.04 . This is mainly for illustration, it does not make sense to speak of an overall gain between the sum of the North ADC's and South ADC's – this should be done separately for each segment.

Pedestals: As can be seen from Figure 2, the algebraic sum over all 36 ADC's for the run for $z = +150$ has negative sums which means pedestal subtracted pulse heights can be negative. In summing the geometric means of the segments, the geometric mean for a segment is computed only if both ADC's are positive, otherwise the ADC's for North and South are simply added. The position of the lower energy peaks for the runs at $z = \pm 150$ are different. Figure 4 shows the spectra for the twice the geometric mean (*mean2*) for the $z = \pm 150$ runs with the $z = +150$ spectrum shifted so the lower energy peaks are aligned. More on pedestals below.

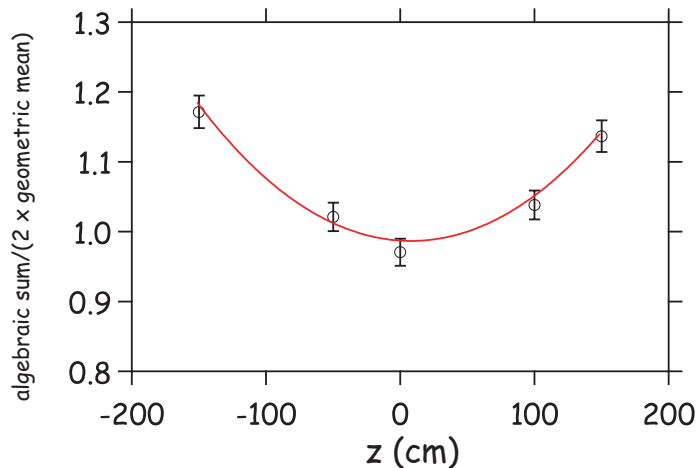


Figure 3: The ratio of the algebraic sum to twice the geometric sum for the North and South sums for the five runs listed in Table 1. The curve is a fit to equation 1 with α given by 1.07 ± 0.04 . This is mainly for illustration, it does not make sense to speak of an overall gain between the sum of the North ADC's and South ADC's – this should be done separately for each segment.

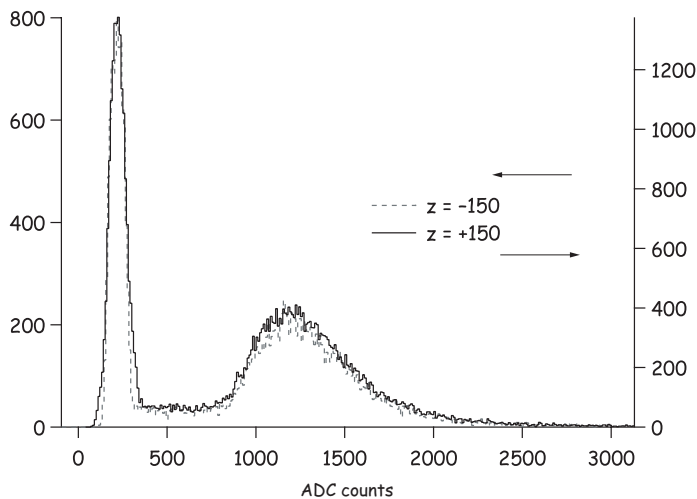


Figure 4: The spectra for the twice the geometric mean (*mean2*) for the $z = \pm 150$ runs with the $z = +150$ spectrum shifted so the lower energy peaks are aligned.

TDC Spectra

In Figure 5 we show the TDC spectra for the five cosmic ray runs. The largest peak in the spectra track as expected but note the spurious peaks. These are most likely instrumental artifacts. Are they understood? In Figure 6 we show the spectra for the $z = \pm 150$ runs for events with total ADC counts below the peak position of the lower energy peak in the ADC spectra. This would seem to indicate that events in the lower energy peak in the ADC spectra are events in which cosmic rays went through a portion of the BCAL module depositing little energy.

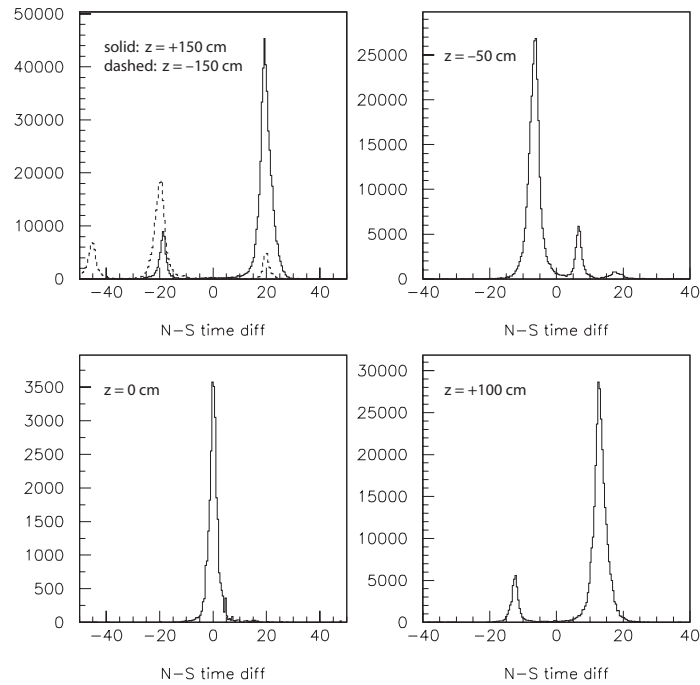


Figure 5: North–South TDC count difference for the five cosmic ray runs. Note the spurious peaks.

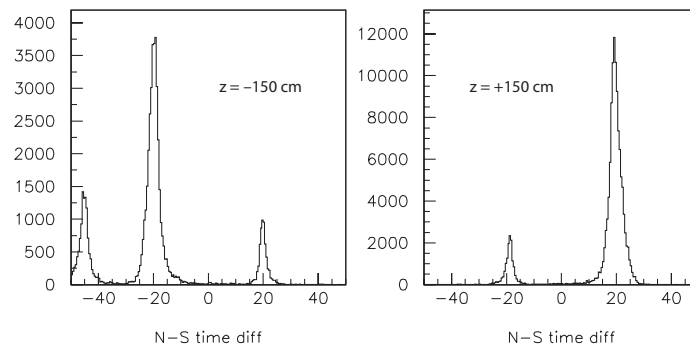


Figure 6: North–South TDC count difference for the five cosmic ray runs for events with total ADC counts below the peak position of the lower energy peak in the ADC spectra.

Near-Far ADC Ratios

Figure 7 shows, for four cosmic ray runs, the ratio of the ADC from the *near* PMT to the *far* PMT for events with ADC values above the lower energy peak. The dashed line indicates the expected ratio based on attenuation effects, *i.e.* $e^{2z/\lambda}$ where $\lambda = 257$ cm.

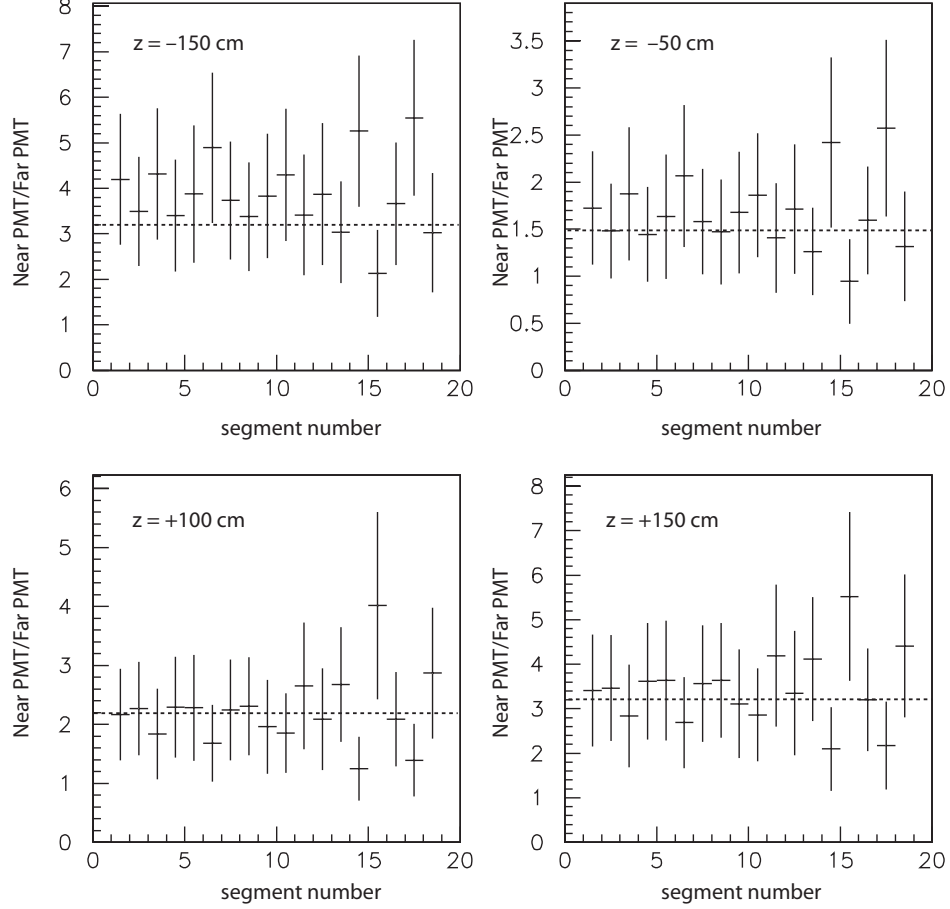


Figure 7: Ratio of the ADC from the *near* PMT to the *far* PMT for events with ADC values above the lower energy peak. The dashed line indicates the expected ratio based on attenuation effects, *i.e.* $e^{2z/\lambda}$ where $\lambda = 257$ cm.

Finding Cosmic Tracks

We look for events associated with a cosmic ray confined to a single layer. These events help us understand the relative gains among segments associated with a layer and then among layers. Figure refmaxlay shows: (a) the fraction of the event energy in the layer with maximum energy; (b) the Index of the layer with maximum energy in the event; (c) the ADC counts for the layer with maximum energy in the event; and (d) the ADC counts for the event when the maximum energy layer contains more than 80% (90%) of the total event energy for $z = -150$ ($z = +150$).

Figure 9 shows the mean ADC for the layer (left) and segments associated with layer (right) as a function of layer index for the layer with maximum energy in the event and when the maximum energy layer contains more than 80% (90%) of the total event energy for $z = -150$ ($z = +150$). The values for both $z \pm 150$ cm track nicely and this information will tell us how to balance the segments among each other.

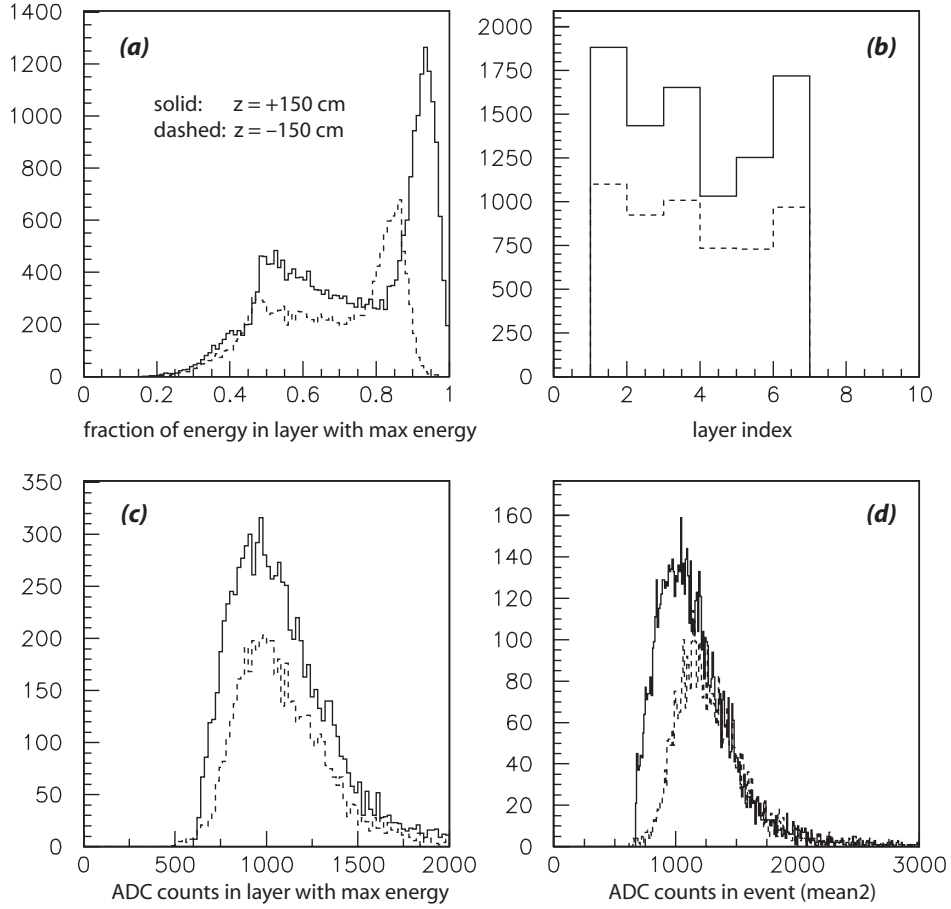


Figure 8: (a) Fraction of the event energy in the layer with maximum energy; (b) Index of the layer with maximum energy in the event; (c) ADC counts for the layer with maximum energy in the event; and (d) ADC counts for the event when the maximum energy layer contains more than 80% (90%) of the total event energy for $z = -150$ ($z = +150$).

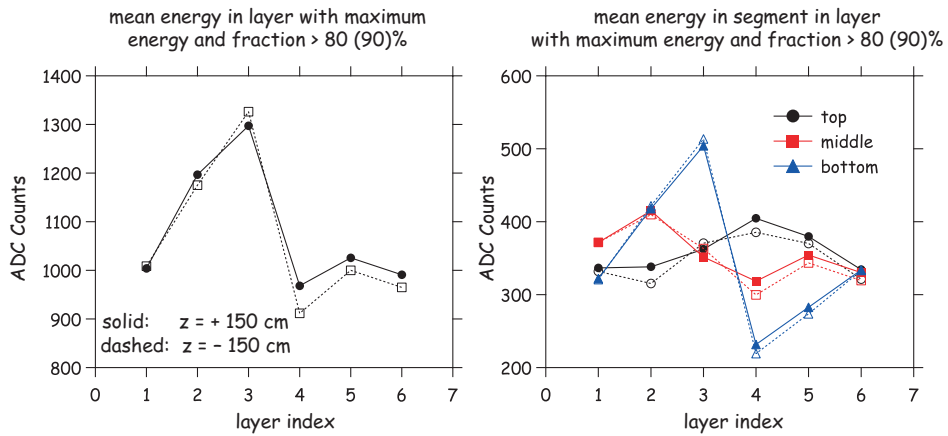


Figure 9: Mean ADC for the layer (left) and segments associated with layer (right) as a function of layer index for the layer with maximum energy in the event and when the maximum energy layer contains more than 80% (90%) of the total event energy for $z = -150$ ($z = +150$).

Monte Carlo Simulation

A toy Monte-Carlo was written to find the energy per segment (18 segments) as shown in Figure 1 and under the assumptions about the cosmic ray paddle placement as described above. The cosmic rays uniformly populated the top paddle with an angular distribution which varied like $\cos^2 \theta$ where $\theta = 0$ for a vertical track. The path length for each track crossing a segment was computed and the assumption made that the deposited energy in the segment is proportional to track length.

Figure 10 shows the integrated path length through the BCAL module for cosmic ray coincidences in the top-bottom paddles as estimated by Monte Carlo. Note the vertical scale is a log scale. The sharp cutoff is at 11.4 cm – the thickness of the BCAL in the vertical dimension. For this simulation, 30% of coincidences have the cosmic ray missing BCAL and 59% have the cosmic ray entering the top and exiting the bottom. The remaining 11% enter the top and exit the side or enter the side and exit the bottom (events between the peak at zero 11.4 in Figure 10) . For the data ($z = +150$ cm), $\approx 58\%$ of the data are in the higher energy peak in the ADC distribution and $\approx 35\%$ in the low energy peak leaving about $\approx 7\%$ in between. These numbers are approximate. If all the cosmic rays were vertical the fraction missing BCAL would be $\approx 33\%$ based on the geometry of the paddles and BCAL. The relative population of the low peak and region between the low peak and high energy peaks in the data clearly depend on the details of the pedestal subtraction.

In Figure 11 we show the ADC distribution for data ($z = +150$ cm) and Monte Carlo. The data use the *mean2* estimate of the total energy. The Monte Carlo distribution results from assuming that a vertical-going minimum ionizing particle traveling through BCAL is equivalent to a 110 MeV photon traversing through the horizontal dimension of BCAL. This is based on the overall calibration from the photon data. The calibration constant is used to convert path length to ADC and then a smearing is applied using the nominal energy resolution obtained from beam data.

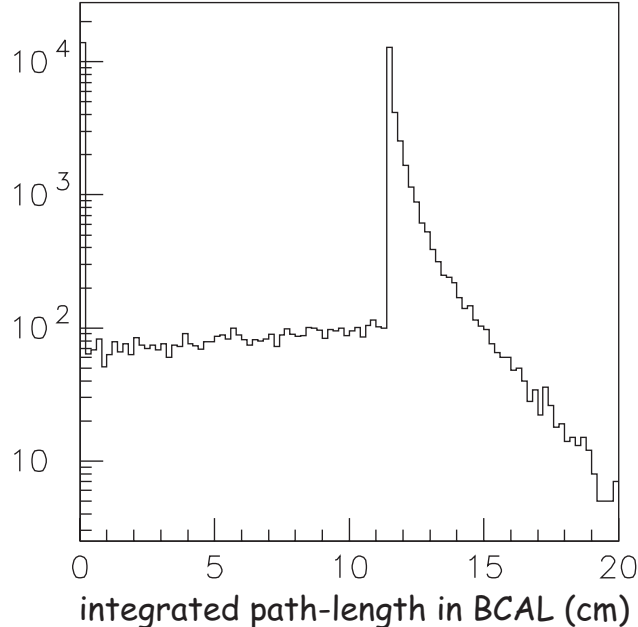


Figure 10: Integrated path length through the BCAL module for cosmic ray coincidences in the top-bottom paddles as estimated by Monte Carlo. Note the vertical scale is a log scale. The sharp cutoff is at 11.4 cm – the thickness of the BCAL in the vertical dimension.

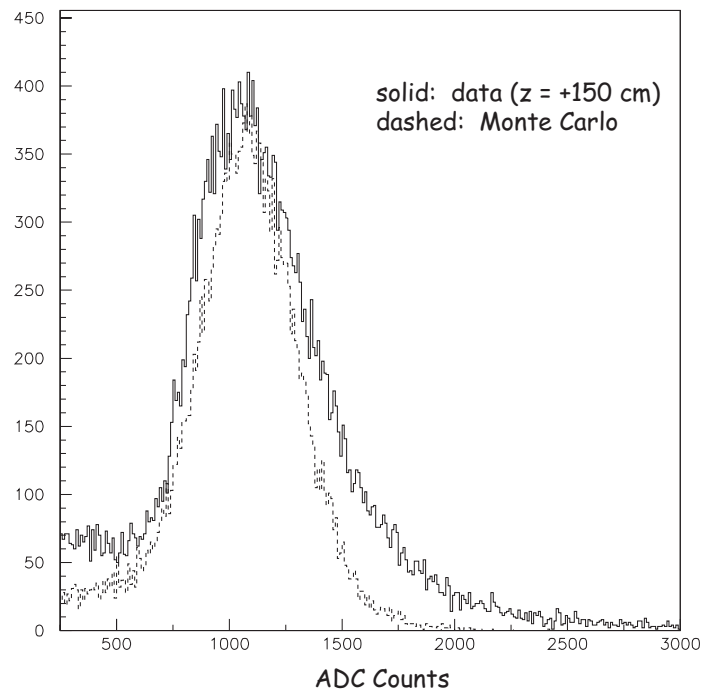


Figure 11: ADC distribution for data ($z = +150$ cm) and Monte Carlo. The data use the *mean2* estimate of the total energy. The Monte Carlo distribution is explained in the text.